Revista Brasileira de Geofísica
RBGf
Brazilian Journal of Geophysics

Revista Brasileira de Geofísica (2014) 32(4): 681-693

ISSN 0102-261X
www.scielo.br/rbg

INFLUENCE OF GRAIN SIZE ON SEISMIC SIGNALS: A PHYSICAL MODELING STUDY

Jhonnes Pin Silva[1], Marco Antônio Rodrigues de Ceia[1], Roseane Marchezi Misságia[1] and Adalto Oliveira da Silva[2]

ABSTRACT. The most common method used worldwide for reservoir characterization is seismic reflection, which is sensible to variations in lithology and fluid content. However, the seismic signals are also affected by pressure, pore geometry and bedding shape. Grain size, especially in unconsolidated sediments, can also influence the propagation of these seismic signals, once it can determine the pore size distribution and porosity. This paper presents a physical modeling study of the variation in seismic responses due to differences in grain size. The experiments were conducted using ultrasonic signals to perform seismic surveys on a Plexiglas block with a wedge-type cavity to simulate a reservoir. Those surveys were conducted with the reservoir filled with four different contents, one containing only the fluid phase and the other three representing an unconsolidated medium characterized by three different grain sizes saturated with the same fluid phase. The results showed how the seismic images, amplitudes, velocities, reflectivities and attenuation can be affected by the grain size.

Keywords: P-wave velocity, unconsolidated media, seismic wave attenuation.

RESUMO. O método mais comumente usado no mundo para caracterização de reservatórios é a sísmica de reflexão, que é sensível a variações na litologia e conteúdo líquido. No entanto, os sinais sísmicos também são afetados pela pressão, geometria dos poros e por outros fatores. O tamanho de grãos, especialmente nos sedimentos inconsolidados, pode também influenciar a propagação destes sinais sísmicos, uma vez que é possível determinar a distribuição do tamanho dos poros e porosidade. Este trabalho apresenta um estudo de modelagem física na variação das respostas sísmicas devido à variação do tamanho de grão. Os experimentos foram conduzidos utilizando sinais de ultrassom para realizar levantamentos sísmicos em um bloco de acrílico com uma cavidade tipo cunha para simular um reservatório. Esses estudos foram realizados com o reservatório preenchido com quatro conteúdos diferentes, um contendo apenas a fase de fluido e os outros três representam um meio não consolidado caracterizado por três granulometrias diferentes saturado com a mesma fase de fluido. Os resultados mostraram como as imagens sísmicas, amplitudes, velocidades, refletividades e atenuação podem ser afetadas pelo tamanho de grão.

Palavras-chave: velocidade de ondas-P, meio inconsolidado, atenuação da onda sísmica.

[1]Universidade Estadual do Norte Fluminense Darcy Ribeiro – UENF, Laboratório de Engenharia e Exploração de Petróleo – LENEP, Av. Brennand s/n, Imboacica, 27925-535 Macaé, RJ, Brazil. Phone: +55(22) 2773-8032/ 2765-6564/ 2765-6561 – E-mail: jhonnes_pin@hotmail.com; marco@lenep.uenf.br; rose@lenep.uenf.br
[2]Faculdade Cenecista de Rio das Ostras-FACRO-CNEC, Rua Renascer da Terceira Idade, Jardim Campomar, 28890-000 Rio das Ostras, RJ, Brazil. Phone: +55(22) 2764-3173 – E-mail: adaltoos@bol.com.br

INTRODUCTION

Seismic responses could vary in different porous media, depending on rock properties, fluid content and enviromental conditions. Bulk density, which depends on porosity, grain and fluid density, is one the main properties that govern the propagation of elastic waves through the rocks, once denser rocks tends to have higher impedances. Gardner et al. (1974) showed that there is a relationship between velocity and bulk density, such a way that velocity increases as density increases. However, the seismic responses also depend on the contrast between elastic impedances of the interfaces and the attenuation of the seismic signals through the layers, which can influence the velocity and amplitude of elastic waves.

The amplitude of the reflected signals depends on several factors such reflectivities of the interfaces, energy loss in each layer, dispersion and wave spreading (Yilmaz, 1987). Grain size can influence those mechanisms and therefore affect velocity and attenuation of seismic waves (Mavko et al., 2009). Both of these properties are frequency-dependent especially for fluid saturated rocks (Batzle et al., 2006).

Early works to study the influence of grain size on seismic signals were conducted using seismic, sonic and ultrasonic waves in marine sediments (McCann & McCann, 1969). Hamilton (1972) used P-waves ranging from seismic to ultrasonic frequencies to perform measurements *in situ* and in lab on unconsolidated marine sediments with different grain sizes. The author also collected data in the literature that were added to his own to form a large database that described the behaviour of velocity and attenuation of compressional waves of different grain sizes. Prasad & Meissner (1992) used pulse transmission techniques to compare laboratory measurements of attenuation in sands to results predicted by Biot theory. Pinson et al. (2008) used the spectral ratio technique to estimate quality factor and the mean grain size from high-resolution seismic data. Park et al. (2009) performed experiments using ultrasonic waves on porous media composed by well sorted glass beads and also verified that grain size can affect the attenuation of the compressional waves.

This paper aims to show how the grain size could affect seismic response in analogue models of pinch-out structures, using physical modeling techniques with seismic ultrasonic reflection surveys in small-scale models and analyzing the influence on the velocities, amplitudes, reflectivities and attenuation. The understanding of such behaviour could be used to make a proper characterization of those structures and advise for the development of modeling algorithms that account for the grain size.

The model consisted of a Plexiglas block with a wedge-type cavity that was filled by four different ways, one containing only brine and other three containing brine and glass beads of different range of grain sizes. For each of the filling cases a 2D common-offset survey was performed, producing very distinct results, such high-resolution images, for a low attenuation media, as poorly detailed images, for highly attenuative media. Attenuation is intrinsecally related to grain size, tending to increase as grain size decreases although it is very low when only the fluid phase fills the cavity. On the other hand, we verified that velocity can vary according to the filling case, even if porosity remains practically the same.

METHOD

The system (Fig. 1) is designed to simulate seismic surveys in geological analogue models in small-scale. It consists of a steel frame, where motorized arms constituted by a set of straps, pulleys and six stepper motors are controlled by a computer that move two transducers (transmitter and receiver) in three dimensions (x, y, z). The transmitter emits an ultrasonic signal that travels through the model whille part of its energy is reflected in the interfaces and capted by the receiving transducer. The electrical signal generated in the receiver is amplified, digitized and stored on a computer using a SEG-Y format, similar to seismic record in the field. The modeling system also includes a data acquisition software developed in LabView platform. This software was designed with a series of panels that allow the configuration of the parameters needed to run the experiment.

The model was made by gluing 9 plates of non-porous Plexiglas material. Later on, a cavity was machined in the resulting block as shown in Figure 2, in order to simulate the edges of a pinch-out reservoir. P-wave velocity for Plexiglas was determined from measurements of the transit time and the thickness of the solid part of the model when placing the transducers directly on it. The result was of 2777 m/s.

The experiments were conducted with constant spacing between source and receiver, and the model was immersed in a water tank. Recordings were taken from the left edge of the model to right edge crossing the reservoir from thicker part towards the thinner. Each survey comprises 151 seismic traces.

The methodology used in this work, which is outlined in Figure 3, consisted in test four different filling cases: the first containing only the fluid phase and the other three representing unconsolidated sediment characterized by three different grain sizes saturated with the same fluid phase.

Initially the reservoir was filled with NaCl brine with salinity of 40 g/l. After it has been fully filled, the model was sealed with a rubber strip and an aluminum plate, pressed by a C-type clamp

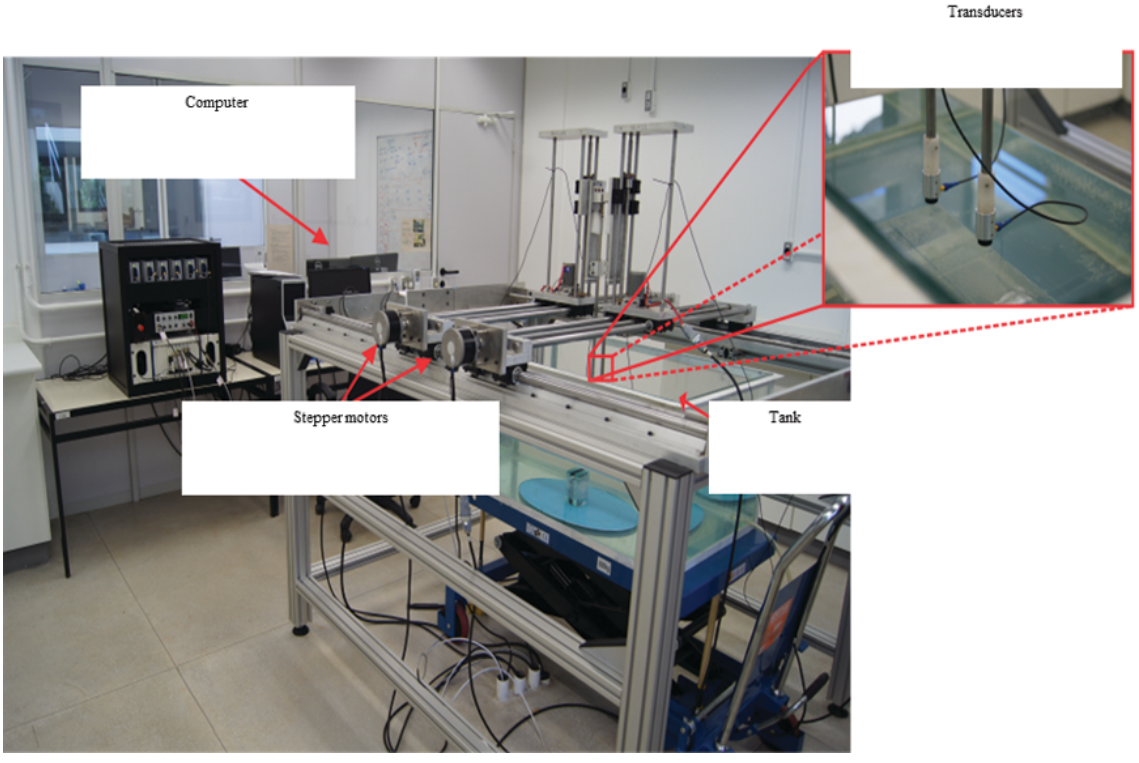

Figure 1 – Experimental setup of the physical modeling system, which consists of PC-driven control unit, a steel frame with a positioning system and piezo-electric transducers.

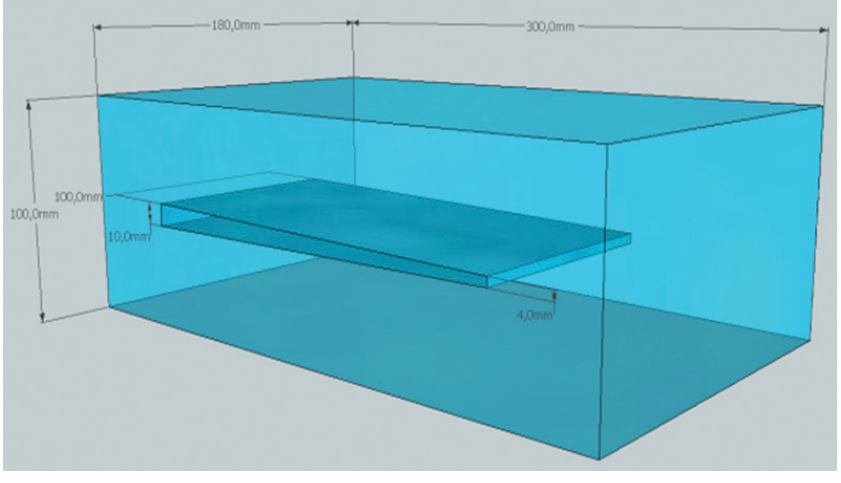

Figure 2 – Schematic of the pinch-out model. Acquisitions were taken from the thicker towards the thinner part.

and placed inside the tank. Then the first survey was performed, producing a SEG-Y file. Later, glass beads were introduced to the reservoir, expelling part of the water, and other surveys were performed for each set of glass beads. Reservoir bulk volume was determined experimentally by measuring the amount of brine used to fill the cavity, which resulted in 140 cm^3. The mass of the glass beads used to fill the cavity was also measured for each set. Glass density was measured using Helium Porosimetry technique (Tiab & Donaldson, 2004) in a matrix cup filled with glass beads. The internal diameter of the matrix cup and the height of glass beads

pack were determined using a digital caliper. Those values allowed calculating the bulk volume of the packs, while the mass of those packs were determined using a digital balance and grain volume measurements were made for each type of the beads. These results allowed estimating an average value of 2.4 g/cm^3 for the grain density. Using that value, it was possible to evaluate the volume of glass beads in the reservoir and therefore the pore volume and porosity. Table 1 shows the porosity values for the different filling cases, which varies within 36-38%. Those values are expected for a random pack of spheres according to Bourbie et al. (1987) (*apud* Molyneux & Schmitt, 2000).

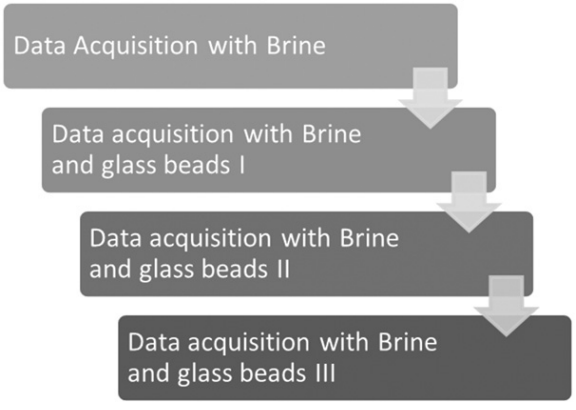

Figure 3 – Work step flowchart. Average particle size of glass beads type I was the smallest, type II had an intermediate size, while type III had the largest size.

Table 1 – Porosity values for the different filling cases.

Filling case	Mass of glass beads (g)	Porosity (%)
Brine + Glass Beads I	206.20	38.63
Brine + Glass Beads II	208.26	38.01
Brine + Glass Beads III	211.90	36.93

The glass beads used to fill the cavity were selected to have particles whose diameter were much smaller than the signal wavelength in order to preserve the fidelity of the model, and avoid generating points of diffraction, whose spreading signal could degrade the seismic image resolution (Misságia & Ceia, 2011). Three particle size ranges (according to the manufacturer) were selected and used. A CILAS 1180 particle analyzer was used to evaluate the particle size distribution and mean diameter (d_m) as show in Figures 4 to 6 and Table 2. That device is based on light diffraction and after placing the samples (brine-saturated glass beads) into the equipment, measurement is possible due to the existence of particles in the optical path of the laser light. This way, the equipment can provide the particle size distribution. The results are reported in Table 2.

Table 2 – Grain size range of the glass beads.

Type	Particle size range (μm)	Mean diameter (μm)
I	200-10	65.79
II	500-30	150.84
III	500-80	278.26

According to Ebrom & McDonald (1994), in seismic physical modeling, a certain feature of a subsurface structure is reproduced in small-scale at laboratory. Typically, for reservoir modeling, thickness is usually put in scale such a way the ratio between wavelength and thickness could be the same such in a real (geological) scale as in the lab. That approach allows simulating seismic surveys on small-scale models in order to investigate the behavior of wave propagation and their implications to seismic imaging and interpretation. Limitations of that methodology includes model reproducibility, differences in source types and wavelets as in the receiver devices, and microscopic features like squirt flow (Mavko et al., 2009) that can affect wave propagation in ultrasonic frequencies.

Contact piezoelectric transducers operating at 500 KHz were used in the experiment, and water depth between the top of the model and the transducers were set to 100 mm. Our experiment was designed assuming a scale of 1:10,000, which corresponds to a water depth of 1000 m in a real marine survey. The same way, the used frequency corresponds to a frequency of 50 Hz in a real survey. Once the available glass beads diameters were in the range of tenths to hundreds of μm, they can represent very coarse conglomeratic material such as large boulders at that scale.

A complete list of the settings used to perform the surveys is presented in Table 3, including sampling rate, period, type of signal and other characteristics.

Table 3 – List of settings used in the experiments.

Setting	Value/Type
Transmitted signal sampling frequency	4,000,000 c/s
Number of samples (transmitted signal)	5,000
Sample length (transmitted signal)	1.25 ms
Signal	Tone Burst
Function window	Bartlett
"Tone Burst" frequency	500 KHz
"Tone Burst" initial phase	0 degree
"Tone Burst" cycles	1
Signal Delay	0 ms

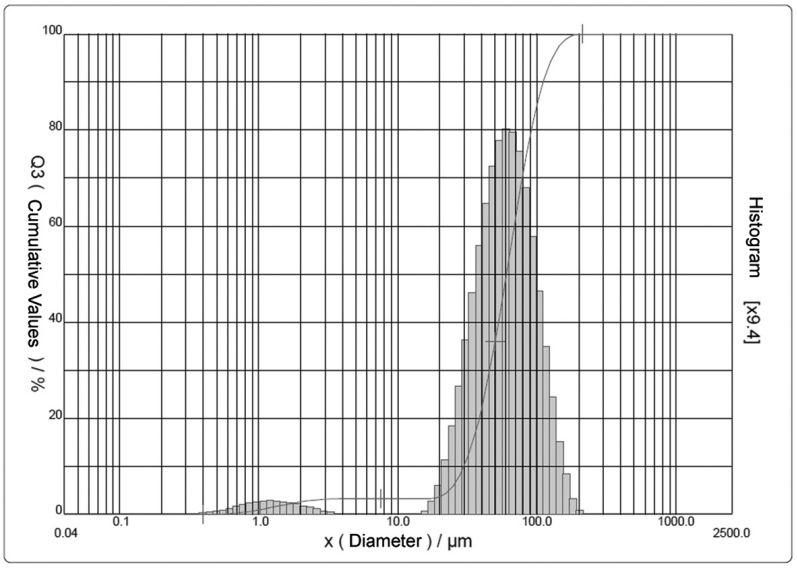

Figure 4 – Particle distribution histogram of glass beads I.

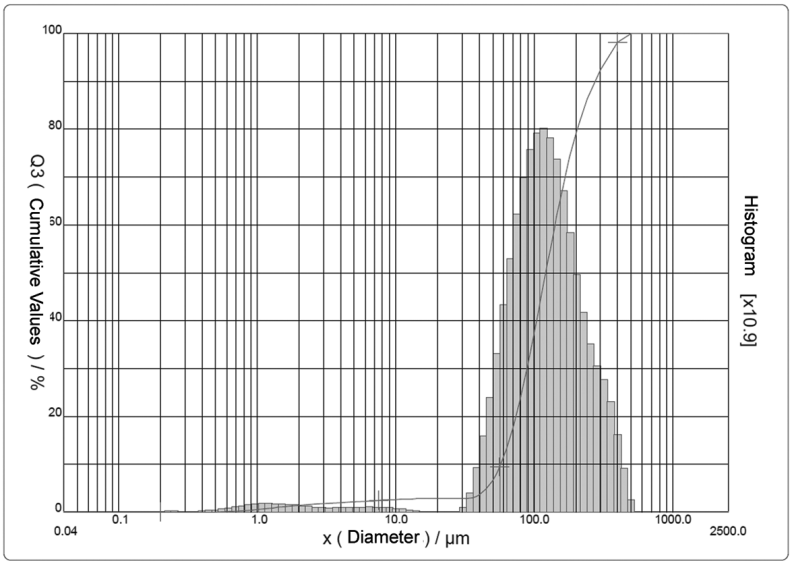

Figure 5 – Particle distribution histogram of glass beads II.

RESULTS

Main features of the model can be observed in Figure 7, which shows the result for the reservoir containing only brine. The top and the bottom of the model (1 and 4) and the reservoir (top '2' and bottom '3'), edge diffractions (6) and a multiple of the top of the model (5) can be easily observed as pointed in the figure.

Figure 8 shows a zoom of Figure 7 focusing on the reservoir. It is possible to observe clearly the top and bottom interfaces, which are very well defined once the attenuation throughout the water seems to have little influence in the signal propagation. That situation did not occur when glass beads are introduced into the reservoir as observed in Figure 9 ($d_m = 65.79\mu$m), Figure 10 ($d_m = 150.84\mu$m) and Figure 11 ($d_m = 278.26\mu$m). In fact, the resolution of those interfaces varies inversely to the grain size.

Using traces from each of the surveys, it is possible to compare and analyze the differences due to the variation in the filling content. Figure 12 shows this comparison for trace 75, obtained at middle of the model. Amplitudes were normalized in respect to maximum amplitude of the individual trace, which is associated to the interface between the top of the model and the water above.

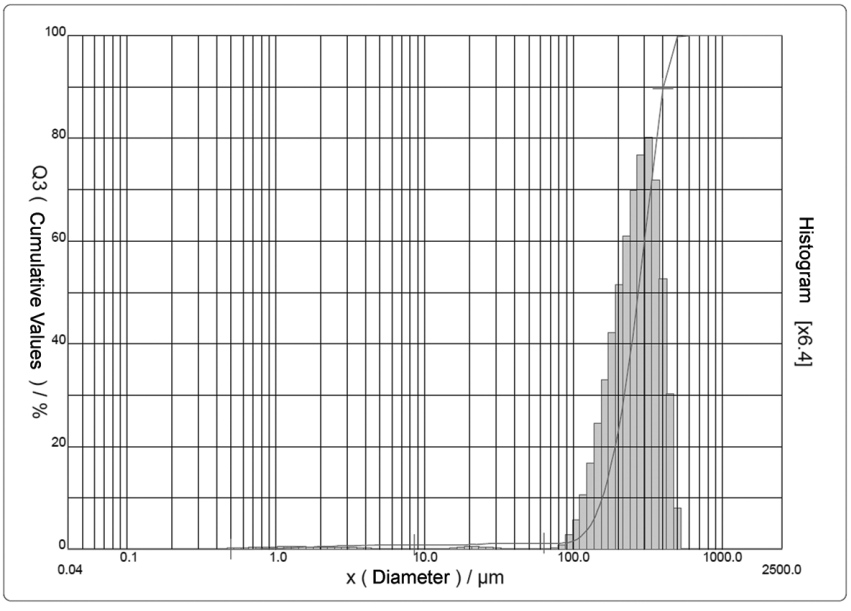

Figure 6 – Particle distribution histogram glass beads III.

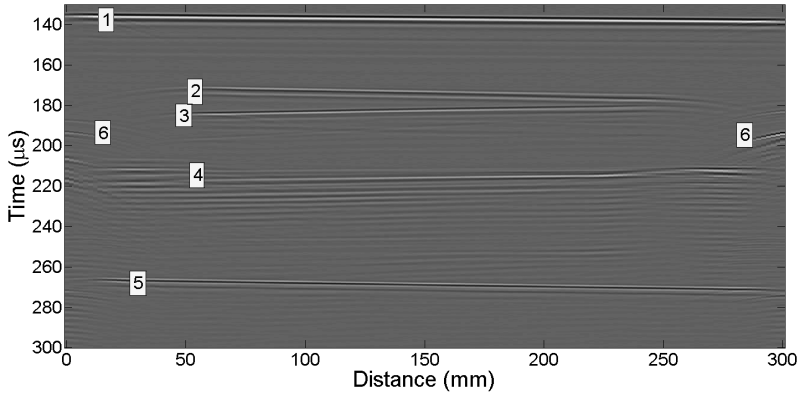

Figure 7 – Seismic image of the physical model with the reservoir filled only with brine.

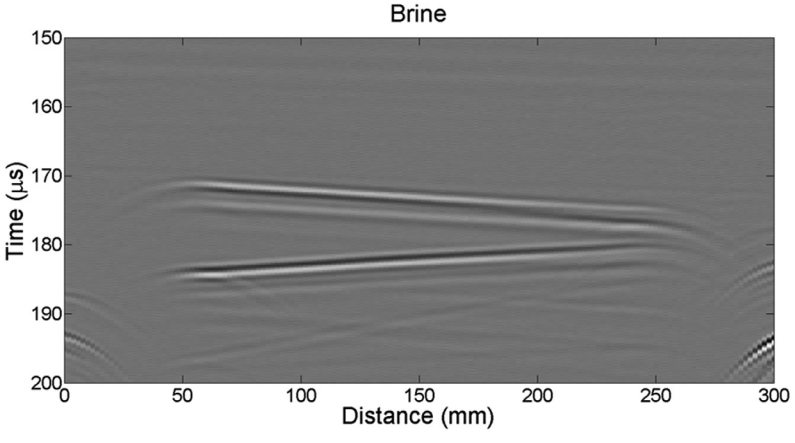

Figure 8 – Seismic image of the physical model with the reservoir filled only with brine. Focus on the reservoir part.

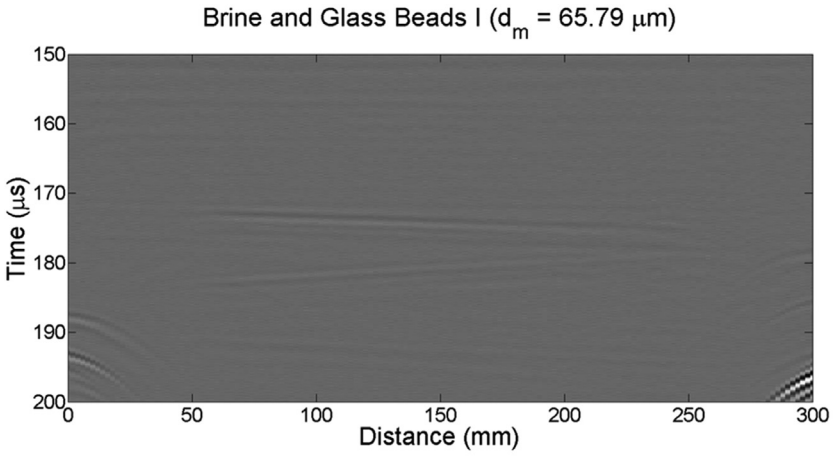

Figure 9 – Seismic image of the physical model with the reservoir filled only with brine and glass beads I ($d_m = 65.79\mu$m). Focus on the reservoir part.

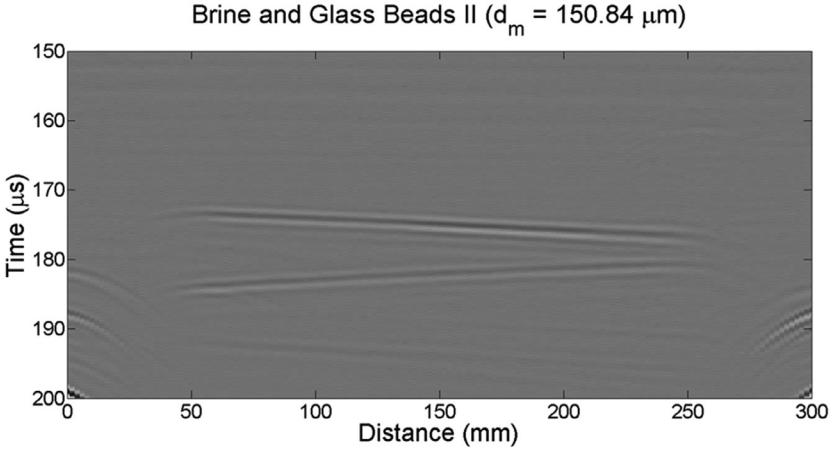

Figure 10 – Seismic image of the physical model with the reservoir filled only with brine and glass beads II ($d_m = 150.84\mu$m). Focus on the reservoir part.

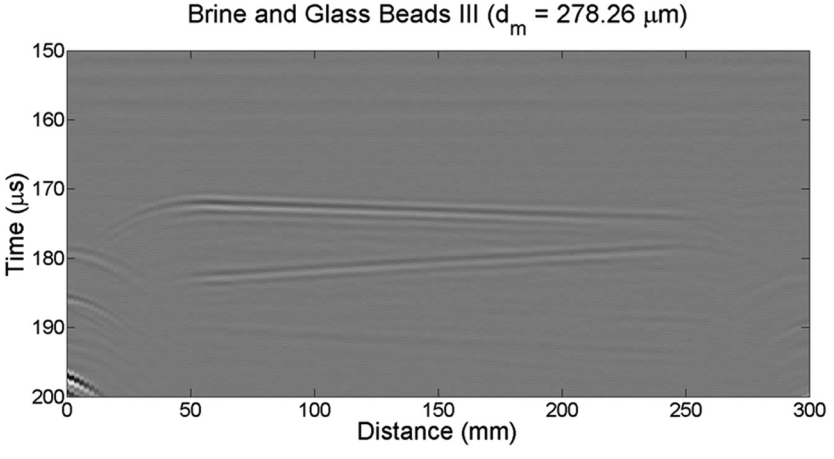

Figure 11 – Seismic image of the physical model with the reservoir filled only with brine and glass beads III ($d_m = 278.26\mu$m). Focus on the reservoir part.

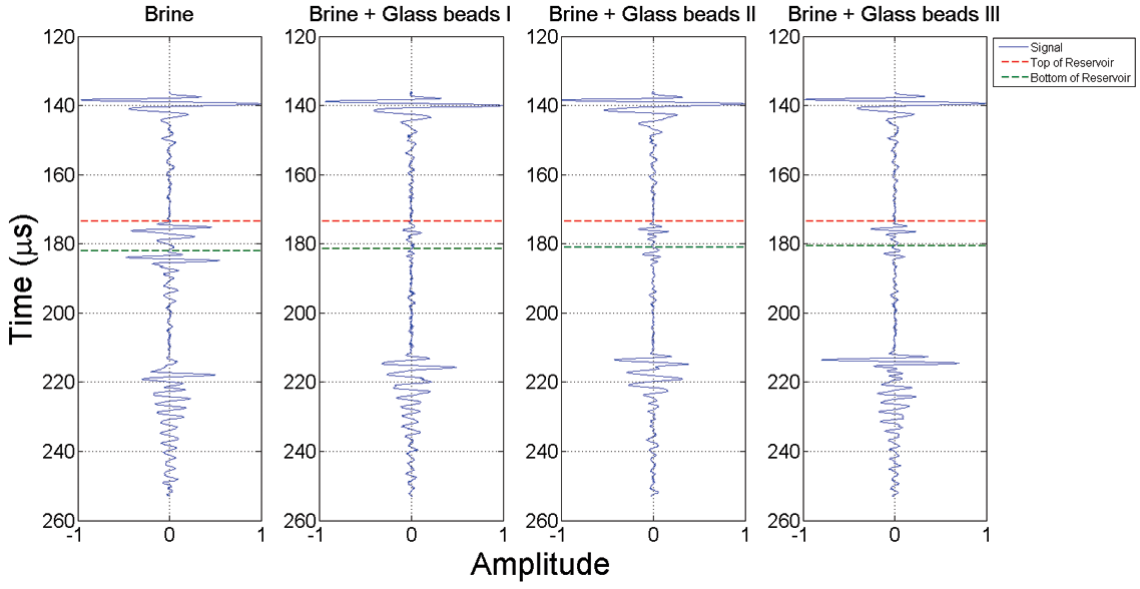

Figure 12 – Seismic trace number 75 that was measured on the middle of the model for different filling contents. Reservoir thickness at this region is 7 mm.

It is possible to verify that the highest amplitudes regarding to the cavity interfaces appeared at the only-brine filling case and the lowest ones for the filling case with the smallest grain size.

Equation (1) could be used to estimate interval velocity of the reservoir:

$$\text{Velocity} = \text{distance/time} \qquad (1)$$

where the distance (or thickness) can be measured at the model and time is obtained from the previous traces (Fig. 9) after associating the peaks to the interfaces that caused those reflections. Table 4 shows the interval velocities for the reservoir in each of the filling cases.

Table 4 – Interval velocity in the reservoir for different filling cases at the middle of the model where the thickness is 7 mm.

Content	Time of the top of reservoir (μs)	Time of the bottom of reservoir (μs)	Velocity (m/s)
Brine	173.5	182.0	1647.058
Glass Beads (type I)	173.5	181.4	1772.152
Glass Beads (type II)	173.5	180.9	1891.892
Glass Beads (type III)	173.5	180.5	2000.000

With the velocity values, a graphic of the interval velocity *versus* average particle size was plotted as shown in Figure 13, which can denote the increment of velocity as grain size increases. Porosities varied very little between the three filling cases of glass beads, in fact, the case using the glass beads III provided the highest porosity, but also the highest velocity.

From the observation of Figure 12, it was also possible to extract and analyze the amplitudes at each reflection. The normalized peak (absolute) values associated to the interfaces are shown in Table 5. This normalization is related to amplitude maximum of the trace in each filling case.

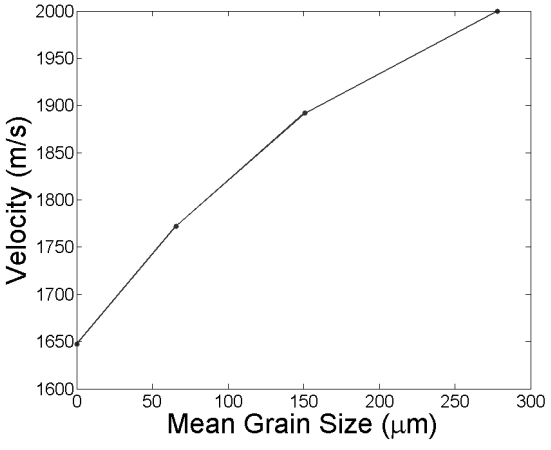

Figure 13 – Graphic of velocities for different grain sizes. Grain size equal to zero refers to the case when only the fluid phase fills the cavity.

In the case of brine-only content, the amplitudes regarded to the top and bottom interfaces have practically the same value, while in the other three cases the bottom interface presents lower values when compared to the top one. The highest amplitude values are related to the brine-only content but for the cases with the glass beads, amplitude tends to increase with the increment of the grain size.

Using the info reported on Table 5 it is possible to plot the normalized peak amplitudes *versus* the mean grain size of the filling cases as shown in Figure 14.

Table 5 – Normalized peak amplitudes for the top and bottom interfaces of the wedge in each of the filling cases (reservoir content).

Reservoir content	Top	Bottom
Brine	0.6071	0.6026
Brine + Glass Beads I	0.0764	0.0550
Brine + Glass Beads II	0.1327	0.0604
Brine + Glass Beads III	0.2243	0.1971

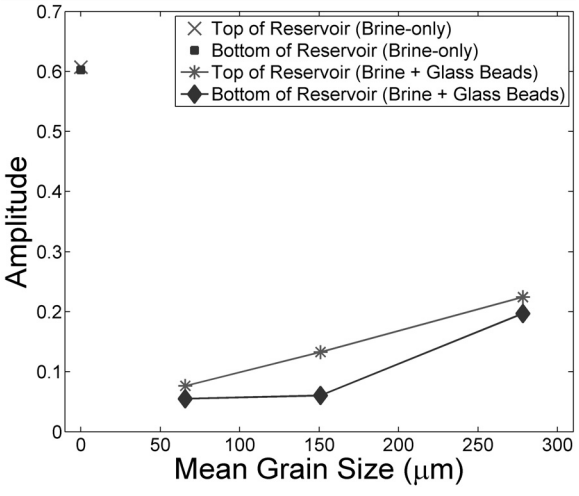

Figure 14 – Graphic of normalized peak amplitudes regarding to the interfaces of top and bottom of the reservoir for different grain sizes.

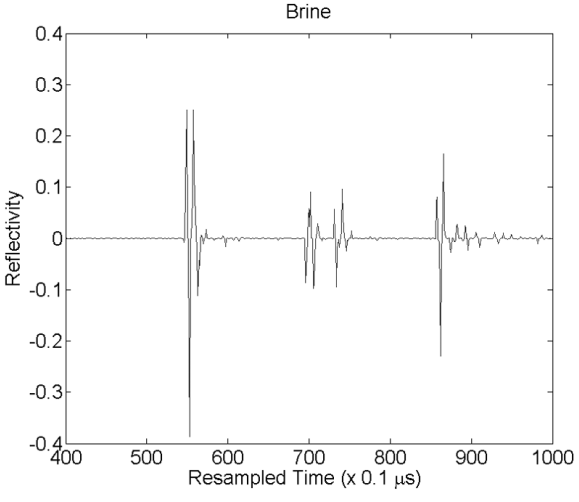

Figure 15 – Reflectivities when the reservoir is filled only with brine.

Another possible analysis is related to the reflection coefficient, which can be found from a data deconvolution. This process can be treated as an inverse filtering process in which the goal is to eliminate the side effects that may have been generated in the data due to the convolutional process (Yilmaz, 1987). Such technique is widely used because it is very simple to be implemented once it is necessary only to inform the wavelet of the source. Figures 15, 16, 17 and 18 show the results for the four filling cases. Those reflectivities were estimated using the method described in Oliveira & Lupinacci (2013).

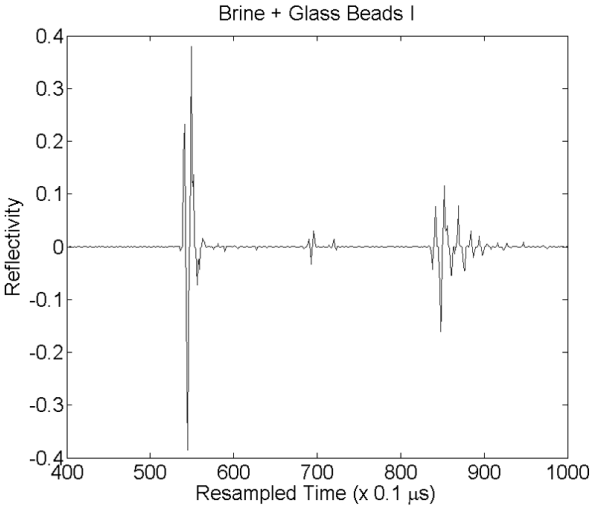

Figure 16 – Reflectivities when the reservoir is filled with brine and glass beads I.

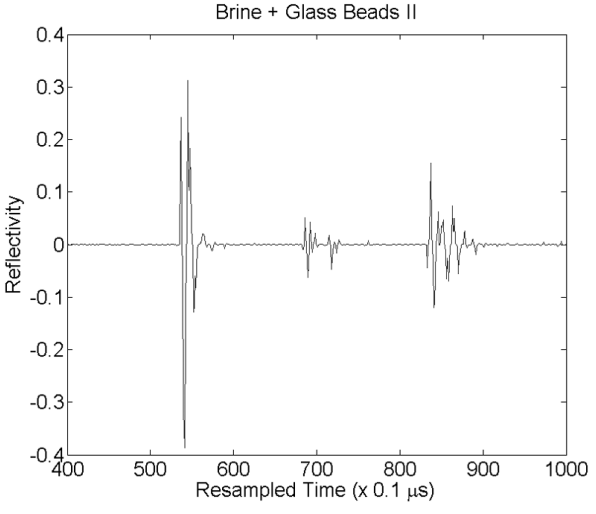

Figure 17 – Reflectivities when the reservoir is filled with brine and glass beads II.

From the reflectivies, it is possible to summarize the absolute values for each interface in each filling case as described in Table 6 and plotted in Figure 19. The first reflectivity is related to the interface between the top of the model and the water above, thus once it is the same for all the situations, it provides the same value. On the other hand, the reflectivities associated to the top and bottom interfaces of the reservoir depend on the filling content. The fluid only case presented an absolute reflectivity of 0.1

whereas for the other cases containing the beads, the reflectivities increase according to the increment of the grain size.

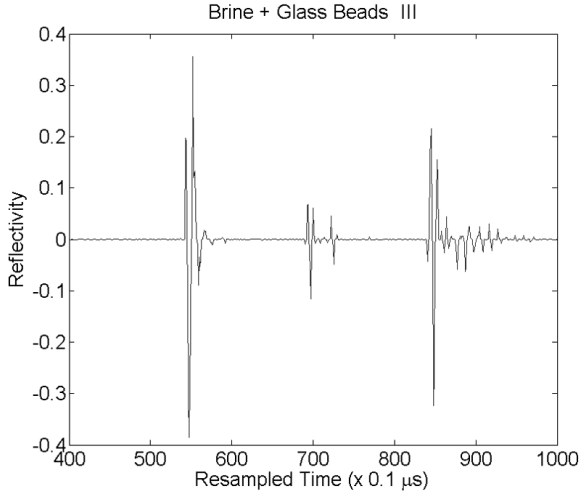

Figure 18 – Reflectivities when the reservoir is filled with brine and glass beads III.

Table 6 – Reflectivity of the interfaces: water-Plexiglas, top of the reservoir and bottom of the reservoir.

Reservoir content	Interfaces		
	water-Plexiglas	Top	Bottom
Brine	0.386	0.098	0.096
Brine + Glass Beads I	0.386	0.032	0.014
Brine + Glass Beads II	0.386	0.062	0.045
Brine + Glass Beads III	0.386	0.116	0.049

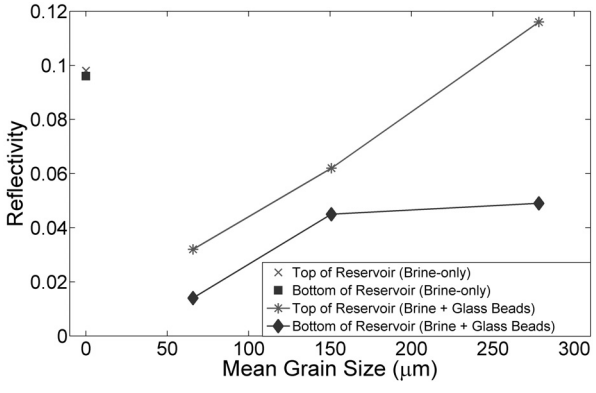

Figure 19 – Variation of the reflectivity according to the grain size.

Q factor at each layer is another property that can be inferred from Figure 12. Within the frequency range of interest, one should calculate the natural logarithm of the ratio between the amplitude spectra of the reference waves. The selection of the frequency band should be in the range of linearity between the amplitude and frequency, thus the slope can be obtained from Eq. (2).

$$slope = \frac{\ln\left(\frac{A(t,f)}{A(t_0,f)}\right)}{f} \tag{2}$$

Knowing that the decay time is $\tau = t - t_0$, one can rewrite Eq. (2) as a function of the slope of the line:

$$Q = -\frac{\pi\tau}{slope} \tag{3}$$

The inverse of Q factor or attenuation was calculated through the Eq. (4).

$$\frac{1}{Q} = -\frac{\ln\left(\frac{A}{A_0}\right)}{\pi f(t - t_0)} \tag{4}$$

Following the described sequence, two intervals of interest are selected with two reflections that will be analyzed, the first interval is first interface and the second interval is the second interface. Figure 20 shows two reflections regarding to the top of the model and the top of the reservoir for the case of brine-only filling. From a direct way, it is possible to obtain the time interval between the two reflections, which was 0.37×10^{-4} μs in that particular case.

Figure 21 shows a graphic of smoothed frequencies for the case of Figure 20. A linear fit is performed, typically in the high frequencies, where high coefficient of determination (R^2) can be achieved. For this case the best band ranges from 4.12 to 4.31 MHz.

From the observation of the slope shown in Figure 22 and the analysis of the coefficient of determination (R^2), it is possible to verify a better adjustment.

The results for the Q factor are shown in Table 7 and the inverse Q is plotted in Figure 23.

Table 7 – Q factor of each layer in each situation.

Reservoir content	Q factor Plexiglas	R^2 (%)	Q factor reservoir	R^2 (%)
Brine	41.67	98	60.06	99
Brine + Glass Beads I	41.11	97	4.90	99
Brine + Glass Beads II	40.42	97	11.88	98
Brine + Glass Beads III	42.41	99	13.92	97.7

CONCLUSIONS

The best resolution of the seismic image of the pinch-out structure occurs when only the fluid phase is filling the reservoir and is characterized by strong amplitudes and well defined contours associated to the top and bottom interfaces. When solid material (glass beads) is added, the resolution vary inversely to the grain

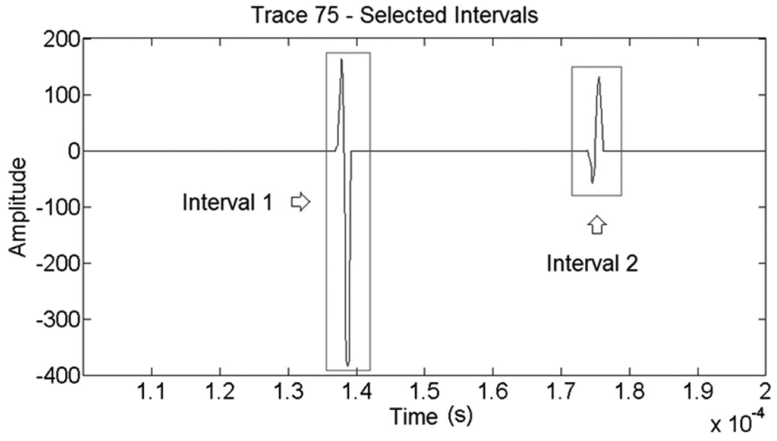

Figure 20 – Selected intervals for spectral analysis in the case of brine content, interval 1 is the top of model and interval 2 is the top of reservoir.

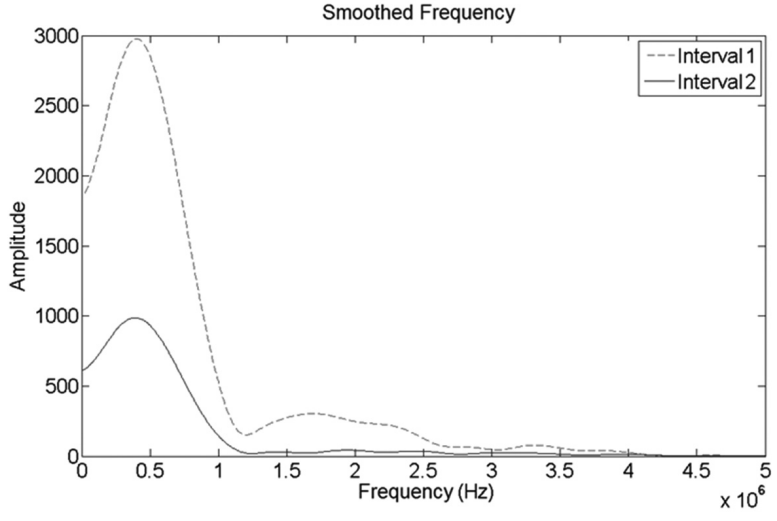

Figure 21 – Smoothed frequency intervals 1 and 2, respectively top and bottom of the reservoir for the same filling case of Figure 20.

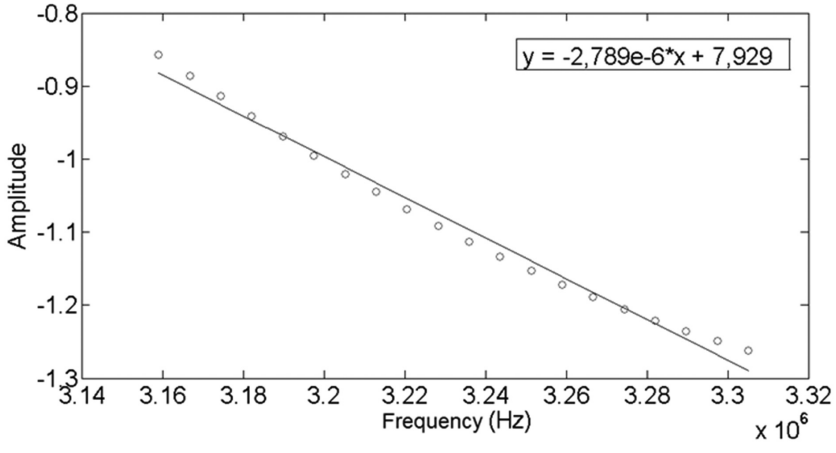

Figure 22 – Linear adjustment with $R^2 = 0.9872$, used to obtain the slope of the line that represents the Q factor.

size, once the delienation of the interfaces, especially the bottom one, becomes more difficult to be observed due to small amplitudes of the reflected signal.

The addition of the glass beads made the top interface reflectivity (absolute values) to decrease significantly in comparison to the only-fluid filling results, but grain size did not affect considerably the observed values. However, the bottom interface reflectivity was severely influenced by the particle size as reported by Hamilton (1972) and Park et al. (2009). In general, the reflectivity of the bottom interface is higher than the top interface one.

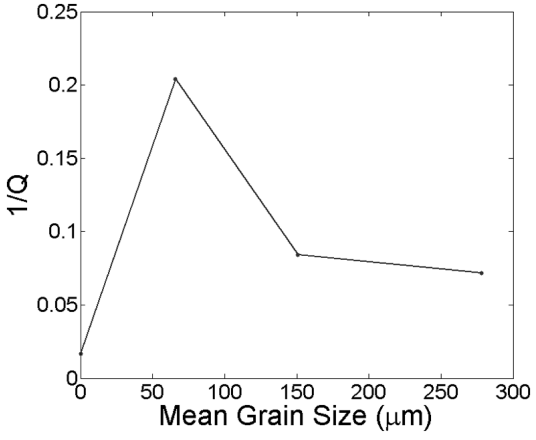

Figure 23 – Variation of the inverse Q factor according to the mean grain sizes.

Velocities were also affected by the glass beads and increase as the size of the grains increases. That behavior can make the top and bottom of the reservoir to get close in the seismograms. Fortunately, both interfaces could be distinguished in all of the seismic images of the experiments. It seems that the interval velocity of the reservoir depends not only on the individual velocities of solid and fluid phases, but also on the number of partitions (grains and pores) along the path from the top to bottom interface. Once there should be fewer partitions when grain sizes increases, velocity tends to be higher for the largest grains (type III). However, for the brine-only case, there were no partitions but the fluid velocity is typically lower than the solids.

The tendency of attenuation, which can be observed by the behavior of the curve of the inverse of Q factor, is to present low values when the reservoir contains only the fluid phase (brine) and to increase as glass beads is added. This variation depends on the particle size since smaller grains cause a higher attenuation of seismic signal as observed by Hamilton (1972). Similar to velocity, partitions (grains and pores) along the path from the top to bottom interface can be a possible cause to the variation in attenuation, once the energy loss also depend on the number of partitions. Nevertheless the brine-only case represented the situation with the fewest number of partitions and this way the least attenuated case.

These experiments were successful to describe how the grain size of the sediments can influence the resolution of seismic images and can be useful in the interpretation of analog structures. In fact, when acoustic properties are used for reservoir characterization of unconsolidated sediments, caution should be taken once relationships to density (Gardner et al., 1974) or porosity (Wyllie et al., 1956) do not account for grain size effects, and can lead to wrongly estimates.

ACKNOWLEDGEMENTS

The authors would like to acknowledge LENEP/CCT/UENF and ANP/PRH-20 for the facilities that made this work possible. JPS thanks CAPES for M.Sc. scholarship. RMM acknowledge FAPERJ for Jovem Cientista research grant. The authors also thank Carlos Andre Assis, Remilson Rosa, Adrielle Silva, Wagner Lupinacci and Irineu Lima Neto for their help during this work.

REFERENCES

BATZLE ML, HAN DH & HOFMANN R. 2006. Fluid mobility and frequency-dependent seismic velocity – Direct measurements. Geophysics, 71(1): N1–N9.

BOURBIE T, COUSSY O & ZINSZNER B. 1987. Acoustics of porous media. Gulf Publ. Co., Editions Technip, Paris, 334 pp.

EBROM DA & McDONALD JA. 1994. Seismic Physical Modeling. Geophysics Reprint Series. No. 15. Society of Exploration Geophysicists, Tulsa, 519 pp.

GARDNER GHF, GARDNER LW & GREGORY AR. 1974. Formation Velocity and density – The diagnostic basics for stratigraphic traps. Geophysics, 39(6): 770–780.

HAMILTON EL. 1972. Compressional-wave attenuation in marine sediments. Geophysics, 37(4): 620–646.

MAVKO G, MUKERJI T & DVORKIN J. 2009. The Rock Physics Handbook. 2nd ed., Cambridge University Press. 503 pp.

McCANN C & McCANN DM. 1969. The attenuation of compressional waves in marine sediments. Geophysics, 34(6): 882–892.

MISSÁGIA RM & CEIA MAR. 2011. Análise do limite da resolução vertical na borda do reservatório: um estudo de Modelagem Física. In: International Congress of the Brazilian Geophysical Society, 12., Expanded Abstracts, 2011, Rio de Janeiro, RJ, Brazil: SBGf, CD-ROM.

MOLYNEUX JB & SCHMITT DR. 2000. Compressional-wave velocities in attenuating media: A laboratory physical model study. Geophysics, 65(4): 1162–1167.

OLIVEIRA SAM & LUPINACCI WM. 2013. L1 Norm inversion method for deconvolution in attenuating media. Geophysical Prospecting, 61: 771–777.

PARK E, LEE K, SEONG W & PARK J. 2009. Sound Speed and Attenuation Measurements in Saturated Glass Beads. In: International Offshore and Polar Engineering Conference. p. 628–632.

PINSON LJW, HENSTOCK TJ, DLX JK & BULL JM. 2008. Estimating quality factor and mean grain size of sediments from high-resolution marine seismic data. Geophysics, 73(4): G19–G28.

PRASAD M & MEISSNER R. 1992. Attenuation mechanisms in sands: Laboratory *versus* theoretical (Biot) data. Geophysics, 57(5): 710–719.

TIAB D & DONALDSON EC. 2004. Petrophysics. Theory and Practice of Measuring Reservoir Rock and Fluid Transport Properties. 2nd edition. Gulf Professional Publishing-Elsevier. 889 pp.

WYLLIE MRJ, GREGORY AR & GARDNER LW. 1956. Elastic wave velocities in heterogeneous and porous media. Geophysics, 21(1): 41–70.

YILMAZ O. 1987. Seismic Data Processing. Society of Exploration Geophysics, Tulsa, 526 pp.

Recebido em 26 setembro, 2013 / Aceito em 19 setembro, 2014
Received on September 26, 2013 / Accepted on September 19, 2014

NOTES ABOUT THE AUTHORS

Jhonnes Pin Silva holds a Petroleum Engineering degree from Faculdade do Espírito Santo (2010) and a M.Sc. in Reservoir and Exploration Engineering in the area of applied geophysics from LENEP/UENF (2013). Currently, works as a Professor at Faculdade do Espírito Santo/ES. Areas of interest: seismic data processing, seismic physical modeling, characterization of physical and mechanical properties of rocks, Petroleum Engineering.

Marco Antônio Rodrigues de Ceia holds a B.Sc. in Physics from the Universidade Federal do Rio de Janeiro (UFRJ), a M.Sc. degree in Geophysics at the MCT-Observatório Nacional and D.Sc. in Exploration and Reservoir Engineering in the area of applied geophysics from LENEP/UENF. Currently, works as Associate Professor of Petrophysics at LENEP/UENF. Areas of interest: Physics of rocks, characterization of physical and mechanical properties of rocks and seismic physical modeling.

Roseane Marchezi Misságia holds a Civil Engineering degree from the Universidade Católica de Minas Gerais – PUC, Belo Horizonte, Brazil, in 1985, a M.Sc. degree in 1988 and a Ph.D. in 2003, in Exploration and Reservoir Engineering in the area of applied geophysics from LENEP/UENF. Currently, works as Associate Professor of Petrophysics at LENEP/UENF. Areas of interest: seismic data processing, seismic physical modeling, characterization of physical and mechanical properties of rocks.

Adalto Oliveira da Silva graduated in Mathematics from Universidade Federal Fluminense (UFF). Holds a M.Sc. degree in Computational Modeling from the Universidade do Estado do Rio de Janeiro (UERJ) and D.Sc. in Reservoir and Exploration Engineering in the area of applied geophysics from LENEP/UENF. Worked as Substitute Professor in the Department of Mathematics of UFF and is currently Professor at SEEDUC/RJ and at the Faculdade Cenecista de Rio das Ostras (FACRO-CNEC) in the Production Engineering course. Areas of interest: seismic data processing, reservoir characterization.